Microelectronics Journal 39 (2008) 1439–1443

Contents lists available at ScienceDirect

Microelectronics Journal

journal homepage: www.elsevier.com/locate/mejo

Application of micro-Raman spectroscopy for the evaluation of doping profile in Zn δ-doped GaAs structures

R. Srnanek [a,*], G. Irmer [b], D. Donoval [a], J. Osvald [c], D. Mc Phail [d], A. Christoffi [d], B. Sciana [e], D. Radziewicz [e], M. Tlaczala [e]

[a] Department of Microelectronics, Slovak University of Technology, Ilkovicova 3, 812 19 Bratislava, Slovak Republic
[b] Institut für Theoretische Physik, Technische Universität Bergakademie Freiberg, Leipziger Street 23, D-09596 Freiberg, Germany
[c] Institute of Electrical Engineering, Slovak Academy of Sciences, Dúbravská cesta 9, 841 01 Bratislava, Slovakia
[d] Department of Materials, Imperial College, London SW7 2BP, UK
[e] Faculty of Microsystems Electronics and Photonics, Wroclaw University of Technology, Janiszewskiego 11/17, 50-372 Wroclaw, Poland

ARTICLE INFO

Article history:
Received 7 March 2008
Accepted 14 June 2008
Available online 22 July 2008

PACS:
78.30.Fs
68.55.Ln
71.55.Eq

Keywords:
Zn delta doping
Concentration profile
Gallium arsenide
Bevel
Raman spectroscopy

ABSTRACT

Micro-Raman spectroscopy was used to characterize beveled Zn delta (δ)-doped GaAs structures. By adapting procedures previously developed for the study of Si δ-doped GaAs structures, Zn-doping profiles were obtained for a set of structures prepared with different doping levels. Values of the doping spike concentration and the full-width at half-maximum of the doping profile were compared with the values obtained by the electrochemical capacitance–voltage (EC–V) and secondary ion mass spectroscopy (SIMS) methods. The good correspondence between this Raman procedure and other well-known methods proves the validity of the technique for determining doping profiles in Zn δ-doped GaAs structures.

1. Introduction

Delta (δ)-doped structures are used in a broad range of semiconductor devices such as field-effect transistors, lasers, light emitting diodes, etc. [1]. Many methods, such as capacitance–voltage (C–V) profiling [2,3], secondary ion mass spectroscopy (SIMS) [4], magneto-transport [5], spectral conductivity [6], photoluminescence [7,8], electro reflectance [9] and others, have been used to determine the position of the doping sheet and the doping profile of the delta-doped layers.

Raman spectroscopy can provide useful information on the characteristic properties of compound semiconductors; thus, the carrier concentration can be quickly determined from the frequency position of L+ longitudinal optical (LO) phonon–plasmon-coupling mode (LOPCM) [10,11]. A disadvantage of this procedure is that it is applicable only for relatively thick semiconductor materials, i.e. for substrates or thick epitaxial layers with the thickness is higher than the penetration depth of the laser light used.

Raman spectroscopy has also been used for the characterization of δ-doped structures. Raman scattering by local vibration modes [12,13] has been used to study the incorporation of Si in single GaAs layers. Samples have been produced in which the doping spike was located at different depths below the surface in different structures. The depth profiles of the Si concentration were obtained qualitatively from the intensity of the local vibration mode of Si (at 384 cm^{-1}) and its dependence on the depth of the doping spike. For samples grown by molecular beam epitaxy, under conditions known to lead to a significant broadening of the doping spike, the Raman technique reveals the incorporation of Si on Ga sites with a broadening of the Si distribution in excess of 20 nm (for a doping level of 8×10^{12} cm^{-2}).

Raman scattering by coupled phonon-inter-sub-band plasmon excitations has also been used for the characterization of Si δ-doped GaAs layers [14,15]. The depth profiling of the layers, using the intensity of a mode appearing at a wavenumber of 282 cm^{-1}, was performed using various lines of the Ar^+ and

* Corresponding author. Tel.: +421 2 60291653; fax: +421 2 65423480.
E-mail address: rudolf.srnanek@stuba.sk (R. Srnanek).

0026-2692/$ - see front matter © 2008 Elsevier Ltd. All rights reserved.
doi:10.1016/j.mejo.2008.06.039

Kr^+ lasers for excitation. Their results yield evidence of the electron localization in the vicinity of the doped sheet and allow the spatial distribution of the electron gas to be estimated.

Both of these Raman methods are restricted to the diagnostics of shallow single δ-doped layers. In our paper [16] a procedure for the direct estimation of the doping spike location and spatial extent of the dopant distribution in Si single and multi-δ-doped layers by micro-Raman spectroscopy was presented. The procedure is based on the evaluation of the transversal optical (TO) and LO phonon intensity ratio along the beveled structure. The observed changes in the Raman spectra were studied and discussed in terms of the coupling between the LO phonon and the photo-excited electron–hole plasma [17,18].

On the basis of our experiences using micro-Raman spectroscopy on beveled samples we have developed a new method [19] of determining the doping concentration profile in GaAs:Si δ-doped structures. The technological challenge of the method is in the preparation of very high-quality bevel surfaces and subsequent scanning by micro-Raman spectroscopy. The doping profile can be measured with very high resolution (e.g. a few nm for Si δ-doped GaAs layers) and can be determined independently of the depth from the surface where other methods are limited, which is very promising for different nanostructures. Standard environmental conditions without the need for complex and expensive ultra-high vacuum systems during the measurement are another advantage of the proposed method.

In this paper we extend the methodology developed for the characterization of n-type δ-doped structures to the study of p-type δ-doped GaAs structures, assessing quantification and extraction of selected properties. We refer to the good agreement between the results from doping profiles determined by complementary methods, namely SIMS and *C–V* profiling.

2. Experimental details

The Zn δ-doped GaAs structures (A, B, C, D) investigated in the present study were grown by metal organic vapor phase epitaxy (MOVPE) on semi-insulating (0 0 1) GaAs substrates. The structures consist of an undoped GaAs buffer layer (500 nm thick) followed by a Zn δ-doped layer capped by an undoped GaAs layer (80 nm). From the duration of the deposition time the Zn sheet concentration of the δ-doped layer was estimated to be in the range of $1.9–4.3 \times 10^{12}\,cm^{-2}$.

To calibrate the micro-Raman measurements obtained for the Zn δ-doped structures a set of five Zn homogeneously doped GaAs layers with different doping concentrations were prepared by MOVPE on semi-insulating (0 0 1) GaAs substrates. The structures consisted of 100 nm-thick Zn-doped GaAs layers, grown on 1000 nm-thick undoped GaAs buffer layers. The doped layers, C1–C5 were grown with carrier concentrations of 1.0×10^{18}, 2.0×10^{18}, 4.0×10^{18}, 7.3×10^{18} and $2.0 \times 10^{19}\,cm^{-3}$, respectively.

The bevels from the test samples and calibration structures were prepared by wet chemical etching in H_3PO_4:H_2O_2:H_2O solution at room temperature [20,21]. We report the very small value of the bevel angle obtained, which was in the range of 10^{-5} rad on all the structures, providing us with very high magnification of the vertical dimensions. Due to the presence of thick oxides of Ga and As on the bevel surfaces on *p*-GaAs created by the etching process, we developed an additional procedure for oxide-free bevel preparation. It involves a careful etching of the samples before and after bevel preparation in 1 HCl:1 H_2O solution. The presence of oxides on the bevel surfaces was controlled by SIMS [22]. During the bevel etching process the samples were kept in darkness, which is a necessary condition for the preparation of high-quality oxide-free surfaces on the bevels.

Before bevel preparation a part of the sample surface was protected by black-wax to be used as a reference surface for measuring the bevel angle. The bevel shape was determined from measurements of the step between the etched and non-etched surface at different positions along the bevel using a step-profilometer. For the characterization of the bevels we have used the definition of bevel magnification *M* from the literature [23], where the value *M* is defined as the reciprocal value of bevel angle expressed in radians and can be obtained by dividing the length along the bevel by the corresponding depth etched into the bulk. The bevels from the calibration structures were prepared with identical magnification of 40,000. The bevels made from δ-doped GaAs structures were prepared with magnifications in the range of 30,000–100,000. Details of the bevel preparation technique were described in our previous works [20,21].

A Jobin Yvon HR800 monochromator equipped with a CCD detector was used to record the micro-Raman spectra at room temperature in the back-scattering geometry. The micro-Raman spectra were excited with a YAG:Nd laser generating the second harmonic line of the wavelength of 532.2 nm. The incident laser beam was focused by a microscope lens to a spot size diameter of 1.8 μm. In order to avoid sample heating the power density of the exciting beam was limited to about $80\,kW/cm^2$.

The structures were examined by electrochemical capacitance–voltage (EC–*V*) profiling. The profiles were measured by a Bio-Rad PN4300PC electrochemical *C–V* profiler at a frequency of 3 kHz. The electrolyte (called as Tiron) was applied to both etch and formed a Schottky contact with the semiconductor being investigated. The area of the Schottky contact was defined by the diameter of the sealing ring. Two different sealing rings, with diameters of 1 and 3.5 mm, were applied.

For the SIMS measurements a physical electronics PHI ADEPT 1010 with a low energy Cs^+ primary ion beam, capable of delivering 100 nA of primary beam current at 750 eV was used.

3. Results and discussion

The Zn δ-doped GaAs structures were beveled and studied by micro-Raman spectroscopy (μ-RS). The laser spot was scanned along the bevel and the μ-RS spectra were recorded and saved. In Fig. 1a there are spectra in different positions marked 1–4 on the bevel. These positions are marked also on the schematic cross-section of the bevel sample in Fig. 1b. Changes of the TO phonon and LO phonon intensities are notable in this figure. For the evaluation of these changes we have registered the variation of the ratio of both intensities, I_{TO}/I_{LO}. Fig. 1c shows the dependence of this ratio along the bevel prepared from structure A. This dependence is characterized by two different characteristics, therefore we have divided this dependence to region I and region II. A border line between these regions lies in the position on the bevel at 6.75 mm. These regions are also marked in Fig. 1b. A similar shape dependence of I_{TO}/I_{LO} along the bevel was observed on the Si δ-doped GaAs structures (Fig. 1b in [19]). We will show that region I of the dependence in Fig. 1c is suitable for the determination of the Zn-concentration profile, as was observed for the Si δ-doped GaAs structures.

Following the procedures in [19] the measured values in region I were fitted by a sigma function (Fig. 2a) followed by its first derivative (Fig. 2b). From the dependence in Fig. 2b we can determine the position of the doping spike D at 79 nm. For determination of the doping profile of the δ-doped layer from its dependence in Fig. 2b it is necessary to use a calibration curve and extracted calibration function. The calibration dependence was obtained (Fig. 2c) by measuring the first derivative of the ratio I_{TO}/I_{LO} along the beveled calibration structures C1–C5. This

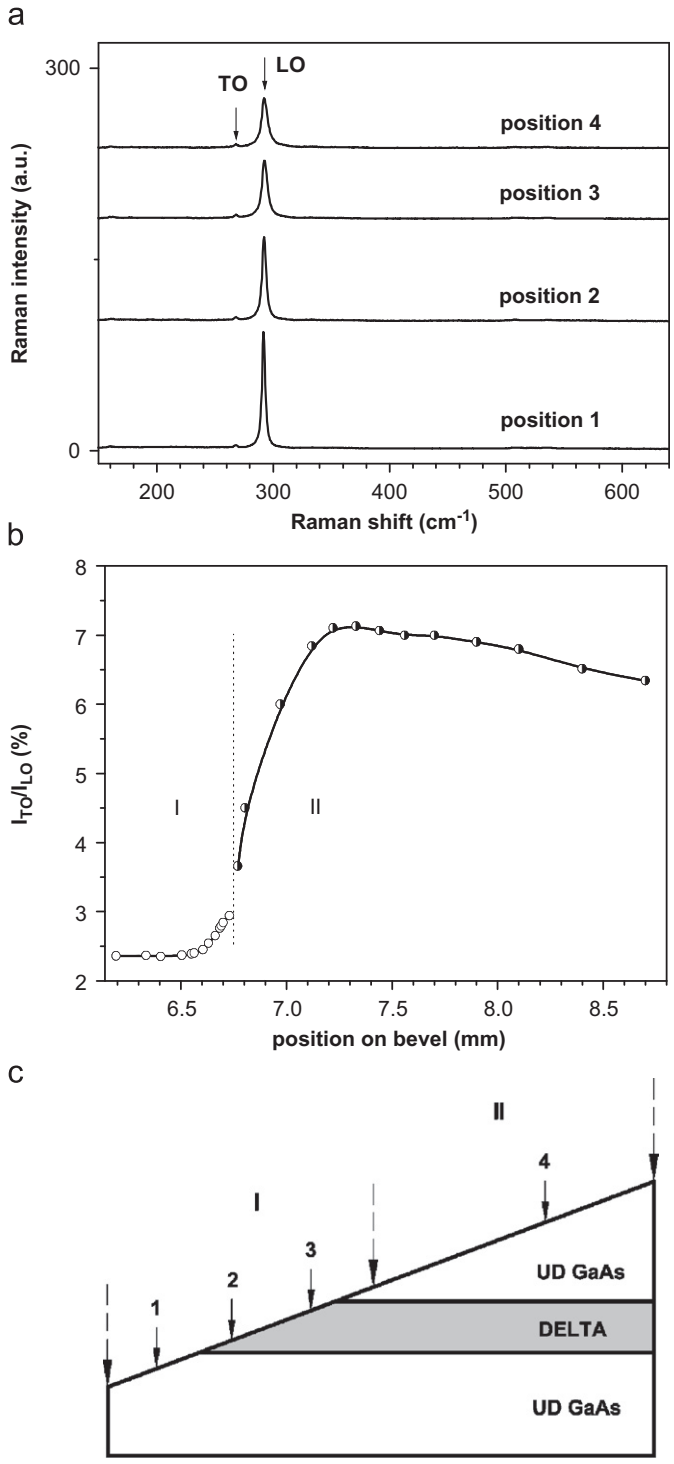

Fig. 1. Study of Zn δ-doped GaAs beveled structure by micro-Raman spectroscopy. (a) Typical micro-Raman spectra recorded along the bevel in different positions 1–4 of laser spot. Labels LO and TO denote the longitudinal optical and transversal optical phonon lines, respectively. (b) The dependence of the ratio of TO and LO intensities along the bevel. (c) A schematic cross-section of the beveled structure. The numbers 1–4 denote the positions of the laser spot on the bevel. Numbers I and II mark the analysed regions. Label UD GaAs denotes undoped GaAs layer.

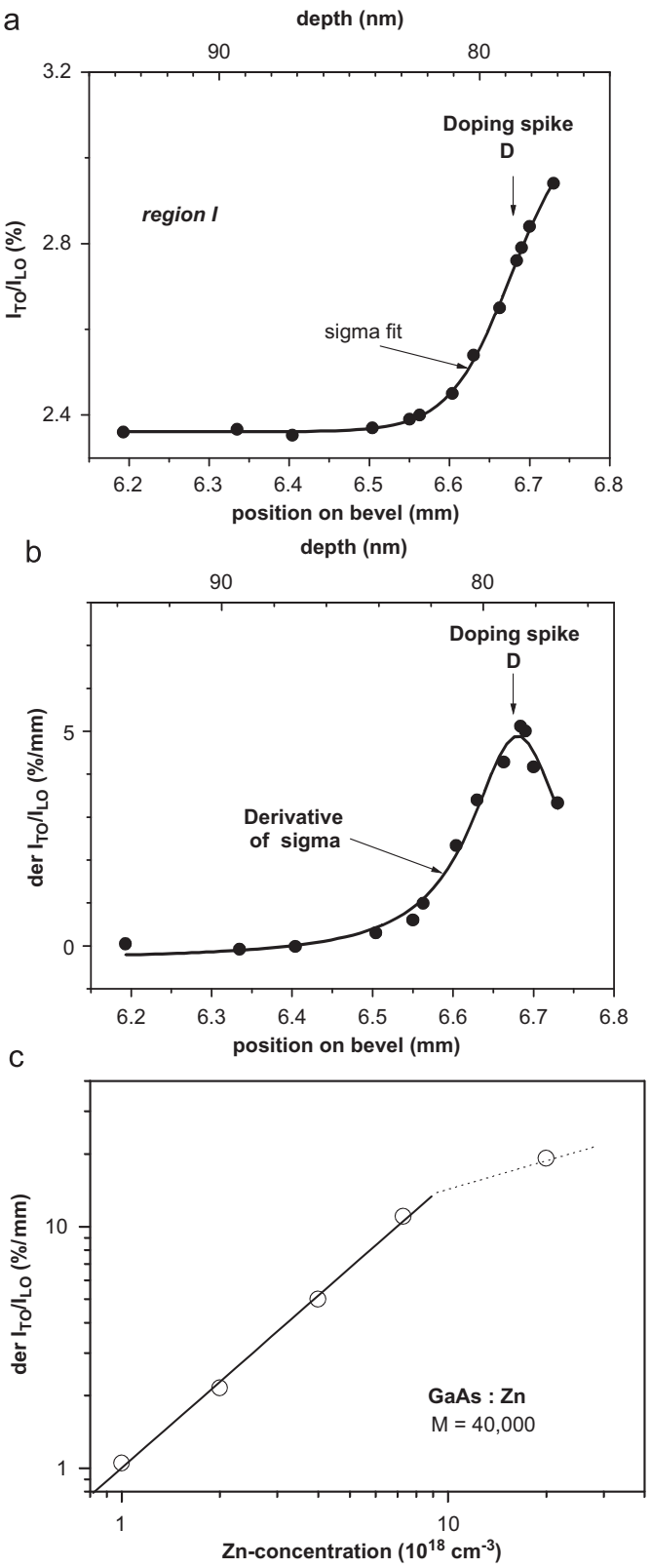

Fig. 2. Steps of Raman procedure to determine the doping profile of studied Zn δ-doped structure. (a) Registration of the ratio of TO and LO intensities, I_{TO}/I_{LO} along the bevel (full dots); fitting of these points by sigma function (line). Labels D denote vertical position of the doping spike in the structure, (b) first derivative of the ratio I_{TO}/I_{LO}. Full points: measured values I_{TO}/I_{LO}. Line: first derivative of the sigma function fitting of experimental values I_{TO}/I_{LO} and (c) calibration dependence obtained from the measuring of the first derivative of I_{TO}/I_{LO} determined along the beveled calibration structures. The bevel magnification, M was identical for all studied structures and it was 40,000.

procedure was described and discussed in detail in our previous work [18,22]. The calibration dependence in Fig. 2c can be fitted well in the range of Zn concentrations of 1–7.3 $\times 10^{18}$ cm^{-3} well by the function

$$\mathrm{der} = -0.9 + 1.6p/\mathrm{E18} \quad (1)$$

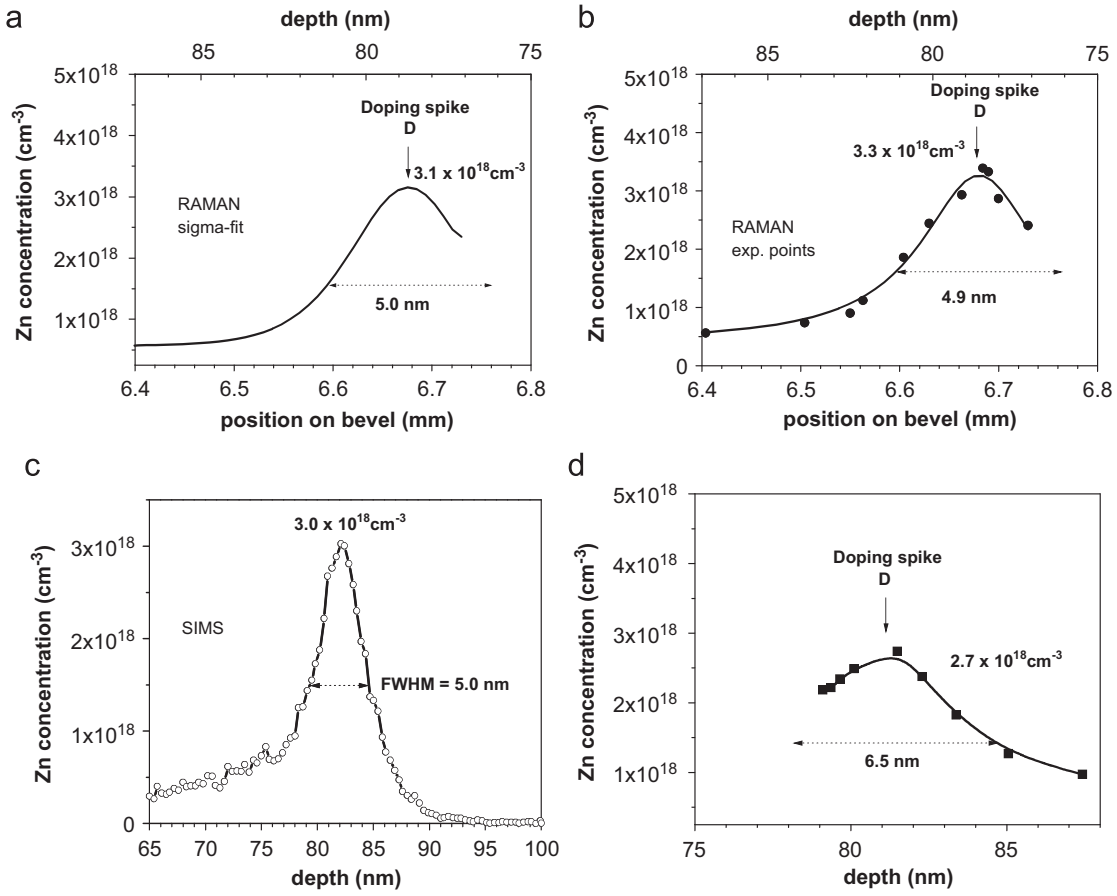

Fig. 3. Zn-doping concentration profile determined in the structure A by using different methods. (a) By presented Raman procedure, that uses sigma fit of experimentally obtained I_{TO}/I_{LO} values and its following first derivative, (b) by Raman procedure that uses direct first derivative of I_{TO}/I_{LO} experimentally obtained values, without using sigma fitting. Obtained discrete values (full points) of doping profile are fitted by Lorentzian function (line), (c) by SIMS method and (d) by EC–*V* method. They are denoted values of doping spike concentration and FWHM of the doping profile in all pictures.

where p is the concentration of Zn in the GaAs layer expressed as 10^{18} atoms cm^{-3} and the value of der = der(I_{TO}/I_{LO}) is expressed in %/mm.

From function (1) we can easily obtain calibration formula (2)

$$p = 0.627(K\,\mathrm{der} + 0.9) \times 10^{18}\,\mathrm{cm}^{-3} \quad (2)$$

where the coefficient K expresses the fact that the bevel angles of the studied δ-doped structure and the calibration structures are different. This coefficient is evaluated as the ratio of bevel angle made from the calibration structure and studied structure, or as the ratio of bevel magnification of bevel made from δ-doped structure, M_δ and calibration structure, M_{cal}:

$$K = M_\delta / M_{cal}$$

By the application of calibration formula (2) on the dependence presented in Fig. 2b (line) we obtain a concentration profile of the Zn atoms in the structure A (Fig. 3a). We have performed comparative measurements by SIMS and *C–V* methods to confirm a validity of the results obtained by the presented micro-Raman method.

In the next two figures, Fig. 3c and d, are concentration profiles obtained by SIMS and EC–*V* methods, respectively. We see that the results (doping spike position in the structure, doping spike concentration and full-width at half-maximum (FWHM) of the obtained doping profile dependence) by the Raman method presented are in good correspondence with the SIMS and EC–*V* methods.

It is known that at a high concentration of doped atoms a lateral diffusion of these atoms is present [1]. The diffusion coefficient of the diffusion from the doping sheet to the direction of substrate and to the direction of surface is different. Some authors [1] observed that the diffusion coefficient in newly grown parts of the layer (direction to the surface) are higher than that in the opposite direction. This behavior can also be seen in Fig. 3c. The concentration profile is therefore non-symmetric and the utilization of the fitting procedure by a sigma function caused some error. When the doping profile is highly asymmetric we can use a modified procedure to evaluate the doping profile. Modification is based on the direct performance of the derivative of the experimental points of I_{TO}/I_{LO}, without fitting by a sigma function. We present this modification in Figs. 2 and 3. In Fig. 2a the experimentally obtained values of I_{TO}/I_{LO} in region I are denoted by full dots. The first derivative of the dependence created from these points is designated in Fig. 2b by full dots. From the dependence presented in Fig. 2b by use of calibration formula (2) we obtain doping concentration profile (Fig. 3b—full dots). After fitting of this dependence by a Lorentzian function the extracted values for the doping spike are 3.3×10^{18} cm^{-3} with a FWHM = 4.9 nm. We see that these values are in sufficient correspondence with the values presented in Fig. 3a. This fact is not surprising because doping profile asymmetricity is observable for doping concentrations lower than about 1×10^{18} cm^{-3} (Fig. 3c). Therefore for structure A the first procedure is adequate and brings sufficiently accurate results.

Table 1
Determined values of doping spike concentration and FWHM of the doping profile in all studied structures A–D by presented Raman method and reference EC–*V* and SIMS methods

Structure, bevel no.	Peak concentration (10^{18} cm^{-3})			FWHM (nm)		
	RAMAN	EC–*V*	SIMS	RAMAN	EC–*V*	SIMS
A, 114	3.1	2.7	3.0	5.0	7.0	5.0
B, 156	5.0	4.0	–	4.4	4.0	–
C, 166	5.9	5.0	–	3.5	3.6	–
D, 120	8.4	8.8	–	4.4	5.0	–

We registered a significant advantage by using the first procedure. By registration of the values I_{TO}/I_{LO} (Figs. 1b or 2a) we can clearly and rapidly detect if the measured value is proper δ-doping profile or is due to the defects or inhomogenities in the structure or on the bevel surface. The values have to follow in region I a sigma function (with a possible small deviation in its shape). When the value of I_{TO}/I_{LO} is changed strongly from the shape of sigma function we have to examine and determine the reason. The atypical value will be once more measured some distance farther from previous measuring position or excluded from discussion. We have experienced that the first presented procedure, which used fitting by a sigma function, causes a smaller error in the estimation of doping spike concentration and FWHM of the concentration profile of dependence than the procedure which uses the direct derivative of experimental values of I_{TO}/I_{LO}. We have therefore for the evaluation of all studied structures used the first presented procedure for all structures A–D. The characteristics values are presented in Table 1. We can ascertain that the values of doping spike concentration and FWHM of doping profile are in good correspondence with other two well-known methods, namely SIMS and EC–*V*. These experiments give us the right to affirm that the Raman method, which was used formerly for n-type δ-doping [19] is convenient also for p-type δ-doping as proved for the case of Zn-doping.

4. Conclusions

We have presented a method of evaluating Zn δ-doped GaAs structures, near a doping spike. Micro-Raman spectroscopy of beveled structures was used. By using and modifying the previously developed procedures for the diagnostics of Si δ-doped GaAs structures Zn-doping profiles were obtained for the set of structures prepared with different doping levels. The results obtained for the doping spike concentration and the spread of doping atoms were compared with SIMS and EC–*V* and a good correspondence was achieved.

Acknowledgements

This work was supported by Slovak VEGA Grants 1/3111/06, 1/0742/08, 2/6097/26 by the Slovak Research and Development Agency under the contract APVV-20-055405, 0655-07, and 51-040605, by Wrocław University of Technology statutory grant, and by the project of Slovak/Poland bilateral cooperation.

References

[1] E.F. Schubert (Ed.), Delta Doping of Semiconductors, Cambridge University Press, Cambridge, 1995.
[2] A. Zrenner, Appl. Phys. Lett. 55 (1989) 156.
[3] E.F. Schubert, J.M. Kuo, R.F. Kopf, J. Electron. Mater. 19 (1990) 521.
[4] R. Badheka, M. Wadsworth, D.G. Armour, J.A. van den Berg, J.G. Clegg, Surf. Interface Anal. 15 (1990) 550.
[5] T.W. Kim, K.S. Lee, Appl. Surf. Sci. 171 (2001) 63.
[6] J. Oswald, J. Pastrnak, F. Karel, O. Petricek, A. Salokatve, Thin Solid Films 342 (1999) 262.
[7] J. Wagner, A. fischer, K. Ploog, Phys. Rev. B 42 (1990) 7280.
[8] R. Srnanek, J. Kovac, R. Kinder, J. Geurts, L. Peternai, D.S. Mc Phail, S. Fearn, R.J. Chater, B. Sciana, D. Radziewicz, M. Tlaczala, Phys. Stat. Sol. (c) 0 (2003) 1055.
[9] A. Drabinska, A. Babinski, T. Tomaszewicz, R. Bozek, J.M. Baranowski, J. Appl. Phys. 92 (2002) 163.
[10] A. Mooradian, A.L. Mc Whorter, Phys. Rev. Lett. 19 (1967) 849.
[11] G. Abstreiter, E. Bauser, A. Fischer, K. Ploog, Appl. Phys. 16 (1978) 345.
[12] J. Wagner, M. Ramsteiner, W. Stolz, M. Mauser, K. Ploog, Appl. Phys. Lett. 55 (1989).
[13] J. Wagner, SPIE conference on spectroscopic characterization techniques for semiconductor technology, SPIE 110 (1992) 1678.
[14] A. Mlayah, R. Carles, E. Bedel, A. Munoz-Yague, Appl. Phys. Lett. 62 (1993) 2848.
[15] A. Mlayah, R. Carles, E. Bedel, A. Munoz-Yague, J. Appl. Phys. 74 (1993) 1072.
[16] R. Srnanek, P. Gurnik, L. Harmatha, I. Gregora, Appl. Surf. Sci. 183 (2001) 86.
[17] R. Srnanek, J. Geurts, M. Lentze, G. Irmer, D. Donoval, P. Brdecka, P. Kordos, A. Förster, B. Sciana, D. Radziewicz, M. Tlaczala, Appl. Surf. Sci. 230 (2004) 379.
[18] R. Srnanek, G. Irmer, D. Donoval, I. Novotny, B. Sciana, D. Radziewicz, M. Tlaczala, Appl. Surf. Sci. 254 (2008) 4845.
[19] R. Srnanek, J. Geurts, M. Lentze, G. Irmer, J. Kovac, D. Donoval, D.S. Mc Phail, P. Kordos, M. Florovic, A. Vincze, B. Sciana, D. Radziewicz, M. Tlaczala, Thin Solid Films 497 (2006) 7.
[20] R. Srnanek, I. Novotny, I. Hotovy, M. El. Gomati, Mater. Sci. Eng. B 47 (1997) 127.
[21] R. Srnanek, G. Irmer, J. Geurts, J. Kovac, D. Donoval, L. Peternai, in: Maria G. Benjamin (Ed.), New Research on Thin Solid Films, Nova Science Publishers, Hauppauge, NY, 2007, pp. 169–210 (ISBN 1-60021-454-1).
[22] R. Srnanek, G. Irmer, D. Donoval, A. Vincze, B. Sciana, D. Radziewicz, M. Tlaczala, Microelectron. J. (2008), in print.
[23] C.M. Hsu, D.S. Mc Phail, Nucl. Instr. Methods Res. B 101 (1995) 427.